References

1. Sobolev V V *Perenos Luchistoi Energii v Atmosferakh Zvezd i Planet* (A Treatise on Radiative Transfer) (Moscow: Gostekhizdat, 1956) [Translated into English (Princeton, NJ: Van Nostrand, 1963)]
2. Chandrasekhar S *Radiative Transfer* (New York: Dover Publ., 1960)
3. Barabanenkov Yu N, Finkel'berg V M *Zh. Eksp. Teor. Fiz.* **53** 978 (1967) [*Sov. Phys. JETP* **26** 587 (1968)]
4. Barabanenkov Yu N *Usp. Fiz. Nauk* **117** 49 (1975) [*Sov. Phys. Usp.* **18** 673 (1975)]
5. Goldberger M L, Watson K M *Collision Theory* (New York: Wiley, 1964)
6. Barabanenkov Yu N, Ozrin V D, Kalinin M I *Asimptoticheckii Metod v Teorii Stokhasticheskikh Lineinykh Dinamicheskikh Sistem (Asymptotic Method in the Theory of Stochastic Linear Dynamical Systems) (Moscow: Energoatomizdat, 1985)*
7. Barabanenkov Yu N, Stainova E G *Opt. Spektrosk.* **63** 362 (1987) [*Opt. Spectrosc.* **63** 211 (1987)]
8. Barabanenkov Yu N, Stainova E G *Opt. Spektrosk.* **59** 1342 (1985) [*Opt. Spectrosc.* **59** 803 (1985)]
9. Barabanenkov Yu N, Kalinin M I *Izv. Vyssh. Uchebn. Zaved. Radiofiz.* **29** 913 (1986) [*Radiophys. Quantum Electron.* **29** 701 (1986)]
10. Lagendijk A, van Tiggelen B A *Phys. Rep.* **270** 143 (1996)
11. Barabanenkov Yu N *Dokl. Akad. Nauk SSSR* **295** 79 (1987) [*Sov. Phys. Dokl.* **32** 556 (1987)]
12. van Hove L *Physica* **21** 517 (1954)
13. Watson K M *J. Math. Phys.* **10** 688 (1969)
14. Barabanenkov Yu N *Izv. Vyssh. Uchebn. Zaved. Radiofiz.* **16** 88 (1973) [*Radiophys. Quantum Electron.* **16** 65 (1973)]
15. Kuga Y, Ishimaru A *J. Opt. Soc. Am. A* **1** 831 (1984)
16. Van Albada M P, Lagendijk A *Phys. Rev. Lett.* **55** 2692 (1985)
17. Wolf P-E, Maret G *Phys. Rev. Lett.* **55** 2696 (1985)
18. van Rossum M C W, Nieuwenhuizen Th M *Rev. Mod. Phys.* **71** 313 (1999)
19. Barabanenkov Yu N, Ozrin V D *Izv. Vyssh. Uchebn. Zaved. Radiofiz.* **28** 450 (1985) [*Radiophys. Quantum Electron.* **28** 305 (1985)]
20. Barabanenkov Yu N, in *Wave Scattering in Complex Media: from Theory to Applications* (Eds B A van Tiggelen, S E Skipetrov) (Dordrecht: Kluwer Acad. Publ., 2003) p. 415
21. Vreeker R et al. *Phys. Lett. A* **132** 51 (1988)
22. Kresin V Z, Ovchinnikov Yu N *Usp. Fiz. Nauk* **178** 449 (2008) [*Phys. Usp.* **51** 427 (2008)]
23. Gulyaev Yu V, Barabanenkov Yu N, Barabanenkov M Yu, Nikitov S A *Phys. Lett. A* **335** 471 (2005)
24. Gulyaev Yu V, Barabanenkov Yu N, Barabanenkov M Yu, Nikitov S A *Phys. Rev. E* **72** 026602 (2005)
25. Barabanenkov M Yu, Barabanenkov Yu N, Gulyaev Yu V, Nikitov S A *Phys. Lett. A* **364** 421 (2007)
26. Barabanenkov Yu N, Barabanenkov M Yu *Elektromagnitnye Volny Elektron. Sistemy* (11) 16 (2007)
27. Vinogradov A P, Dorofeenko A V, Zouhdi S *Usp. Fiz. Nauk* **178** 511 (2008) [*Phys. Usp.* **51** 485 (2008)]
28. Ambartsumyan V A *Zh. Eksp. Teor. Fiz.* **13** 244 (1943)
29. Barabanenkov Yu N, Kouznetsov V L, Barabanenkov M Yu *Prog. Electromagn. Res., PIER* **24** 39 (1999)
30. Barabanenkov Y N, Barabanenkov M Y, in *PIERS 2006: Progress in Electromagnetics Research Symp., March 26 – 29, 2006, Cambridge, Mass., USA: Proc.* (Cambridge, Mass.: The Electromagnetics Academy, 2006) p. 10
31. Reid W *Indiana Univ. Math. J.* **8** 221 (1959)
32. Redheffer R *Indiana Univ. Math. J.* **8** 349 (1959)
33. Dorokhov O N *Pis'ma Zh. Eksp. Teor. Fiz.* **36** 259 (1982) [*JETP Lett.* **36** 318 (1982)]; *Solid State Commun.* **44** 915 (1982)
34. Mello P A, Pereyra P, Kumar N *Ann. Physics* **181** 290 (1988)
35. Klyatskin V I *Metod Pogruzheniya v Teorii Rasprostraneniya Voln* (Embedding Method in the Wave Propagation Theory) (Moscow: Nauka, 1986)
36. Barabanenkov Yu N, Kryukov D I *Waves Random Media* **2** (1) 1 (1992)
37. Mello P A, Stone A D *Phys. Rev. B* **44** 3559 (1991)
38. Yablonovitch E *Phys. Rev. Lett.* **58** 2059 (1987); John S *Phys. Rev. Lett.* **58** 2486 (1987)
39. Barabanenkov Yu N, Barabanenkov M Yu *Zh. Eksp. Teor. Fiz.* **123** 763 (2003) [*JETP* **96** 674 (2003)]
40. Barabanenkov Yu N, Kalinin M I *Phys. Lett. A* **163** 214 (1992)
41. Gazaryan Yu L *Zh. Eksp. Teor. Fiz.* **56** 1856 (1969) [*Sov. Phys. JETP* **29** 996 (1969)]
42. Anderson P W *Phys. Rev.* **109** 1492 (1958)
43. Gertsenshtein M E, Vasil'ev V V *Teor. Veroyatn. Ee Primen.* **4** 424 (1959) [*Theor. Probab. Appl.* **4** 391 (1959)]

PACS numbers: **41.20. – q**, 42.65.Pc, **85.50. – n**
DOI: 10.3367/UFNe.0179.200905i.0539

Local fields in nanolattices of strongly interacting atoms: nanostrata, giant resonances, 'magic numbers,' and optical bistability

A E Kaplan, S N Volkov

S M Rytov took an interest in many things, including the theory of layered media with a period much smaller than the wavelength [*Zh. Eksp. Teor. Fiz.* **29** 605 (1955)]. One of us, A E K, who participated in Rytov's seminars for 20 years, until 1979, was also involved with multiple and various things, and was sometimes surprised to realize that his work touches upon old areas of interests of Rytov. Of course, there is little surprise here, because Rytov had an intuition for unusual and fundamental things, and he often looked far ahead. Our new results presented here echo, to an extent, those old interests of Rytov.

In this report, following our recent brief publication [1], we consider a number of new effects emerging in one- and two-dimensional ordered systems of two-level atoms with a sufficiently strong dipole interaction. We have shown that in systems smaller than the wavelength of light, an excitation of the atomic dipole moments may become substantially inhomogeneous, forming strata and two-dimensional structures of a nanometer scale. Such behavior of the local field in a dielectric system is significantly different from the results of the Lorentz–Lorenz theory for local fields; it gives rise to resonances defined by the size and geometry of the system and is capable of inducing a giant local-field enhancement. We demonstrated that the saturation nonlinearity in two-level atoms may cause optical bistability, in particular, in the simplest case where the system is comprised of two atoms only. We also predicted 'magic' system sizes and geometries that, unlike the Lorentz model, do not result in a suppression of the local field in the system when the laser frequency is tuned to the resonance of the two-level atom.

A known fact of the electrodynamics of continuous media is that the microscopic field acting on atoms or molecules (known as the 'local field') is generally different from the macroscopic (average) field because of the dipole interaction between the particles composing the medium. This difference is a central point of the classical theory of local fields in dielectrics advanced by Lorentz and Lorenz [2]. An important, albeit implicit, assumption of that theory is that the local field remains virtually unchanged from atom to atom over distances much shorter than the wavelength of light λ. The theory is therefore essentially based on the so-called 'mean-field approximation.'

Rapid advances in nanotechnology opened up possibilities of fabricating artificial systems of strongly interacting particles, for which the assumption of the local-field uniformity is no longer valid. It is natural to presume that abandoning the mean-field approximation in the description of the local fields may result in a discovery of many new and interesting phenomena, just as passing from the macroscopic Curie–Weiss theory to the Ising model significantly extended the ability of the theory to describe magnetic materials [3]. Of course, this does not mean that a complete analogy is to be expected in the descriptions of local fields and magnetic media. In our case, even more interesting discoveries can be expected because the atomic electric dipoles induced by the local fields are driven by an incident electromagnetic wave, in contrast to the static magnetic dipoles in the Ising model. Another crucial distinctive feature of our work is that the systems under consideration are very small, less than the wavelength in size, while the majority of studies in the theory of magnetism focus on building a macroscopic, 'thermodynamic,' description of the medium.

In this report, based on the results initially presented in our recent brief publication [1], we demonstrate that accounting for significant spatial variations of the local field from atom to atom, on a scale much less than the wavelength, opens the way for describing many new effects in ordered systems of strongly interacting atoms, including giant local-field resonances, 'magic' system sizes and geometries, and optical bistability and hysteresis. Of particular importance is that our research brings forward a totally new paradigm in the theory of light–matter interaction. Our calculations show that various field-related and array-related factors may disrupt a smooth variation of the local field from atom to atom, giving rise to nearly periodic strata or more complex patterns of induced dipole moments. They are most pronounced in one- and two-dimensional dielectric systems comprising atoms, molecules, quantum dots, clusters, or other resonant particles. The resonant nature of the interaction between the particles allows controlling the anisotropy and strength of the interaction. If the light wave then propagates normally to the one- or two-dimensional lattice, we can also eliminate wave propagation aspects of the problem.

In general, two major types of dipole strata emerge: short-wave, with the period up to four interatomic distances, and long-wave strata. The strata can be interpreted as standing waves of local-field excitations, which we hereafter call 'locsitons.' The locsitons are electrostatic by nature and can have a very low group velocity. They may be classified as Frenkel excitons [4] because the electrons are bound to the atoms and there is no charge transfer in the systems under consideration.

In the first approximation, the phenomenon under consideration is linear in the external field, and locsitons can be excited within a spectral band much broader than the atomic linewidth. It essentially amounts to a Rabi broadening of a spectral line of a resonant atom, which arises because of strong interatomic interactions. The dipole strata can be controlled by adjusting the laser polarization and the dimensionless interatomic coupling parameter Q (see below), which depends, in turn, on the interatomic distance, on the dipole moment and spectral linewidth of the resonant transition in the atoms, and on the detuning of the laser frequency from the atomic resonance. For $|Q| > Q_{\rm cr} = O(1)$, the smooth variation of the local field from atom to atom can be broken by boundaries, impurities, defects in the lattice, etc. A most striking manifestation of the effect is the emergence of large local-field resonances due to locsiton eigenmodes in finite arrays and lattices. Another interesting and unexpected phenomenon is an almost complete cancelation of the local-field suppression if the laser frequency is tuned exactly to the atomic resonance and the system is comprised of a certain 'magic' number of atoms. Moreover, in a system with a saturation nonlinearity, different types of optical bistability and hysteresis can emerge.

Our model is based on the dipole interaction between atoms. We can neglect retardation effects because of the small size of the system; therefore, similarly to the classical theory of local fields [2], we rely on the fact that the near field of a dipole is predominantly quasistatic and nonradiative in nature. The frequency ω of the incident laser radiation is close to the resonant frequency ω_0 of the atom, which we approximate by a two-level system [5–7] with a transition dipole moment $d_{\rm a}$. The local field acting on an atom at a point $\mathbf{r}$ can be represented as a sum of the field $\mathbf{E}_{\rm in}$ of the light wave incident on the system and the quasistatic contributions from all other dipoles (with their coordinates denoted as $\mathbf{r}'$) that are induced by the local fields $\mathbf{E}_{\rm L}(\mathbf{r}')$:

$$\mathbf{E}_{\rm L}(\mathbf{r}) = \mathbf{E}_{\rm in}(\mathbf{r}) - \frac{Q}{4}\sum_{\rm lattice}^{\mathbf{r}'\neq\mathbf{r}} \frac{l_{\rm a}^3}{|\mathbf{r}'-\mathbf{r}|^3} \times \frac{3\mathbf{u}[\mathbf{E}_{\rm L}(\mathbf{r}')\,\mathbf{u}] - \mathbf{E}_{\rm L}(\mathbf{r}')}{1+|\mathbf{E}_{\rm L}(\mathbf{r}')|^2/[E_{\rm sat}^2(1+\delta^2)]}\,, \tag{1}$$

where $\mathbf{u}$ is the unit vector along $\mathbf{r}-\mathbf{r}'$, $\delta = T\Delta\omega = T(\omega-\omega_0)$ is the dimensionless detuning of the laser frequency from the atomic resonance, and $E_{\rm sat}^2 = \hbar^2\varepsilon/(|d_{\rm a}|^2\tau T)$ is the saturation intensity of the two-level system. The dimensionless coupling parameter

$$Q = \frac{4|d_{\rm a}|^2 T}{\varepsilon\hbar l_{\rm a}^3(\delta+{\rm i})} \tag{2}$$

represents the strength of the dipole interaction between neighboring atoms. The coupling parameter and the saturation intensity depend on the transverse relaxation time $T = 2/\Gamma$ of the two-level atom, whose homogeneous spectral linewidth is Γ, on its longitudinal relaxation time (excitation life time) τ, and on the background dielectric constant ε. We also assume that the interatomic distance $l_{\rm a}$ is large enough to prevent any overlap between atomic orbitals of neighboring atoms, $l_{\rm a} \gg |d_{\rm a}|/e$. This assumption is, in fact, also present in the standard Lorentz theory of local fields [5–7], in which the interaction between atoms and molecules is treated classically. Our approach radically departs from the standard Lorentz theory in that we do not assume any averaging of the local field over the neighboring sites of the crystalline lattice, which would reveal itself in the assumption that $\mathbf{E}_{\rm L}(\mathbf{r}) = \mathbf{E}_{\rm L}(\mathbf{r}')$, and we do not use an encapsulating sphere around the observation point, outside which a continuous medium is assumed.

Large transition dipole moments, for example, in alkali vapors, CO_2, narrow-band resonances in solids [9], quantum dots, and clusters may significantly enhance the effects that we discovered. In many of these cases, locsitons can emerge with $l_{\rm a}$ as large as a few tens of nanometers. We note that surface plasmons in metal–dielectric composites [10, 11] usually require a more sophisticated theoretical description

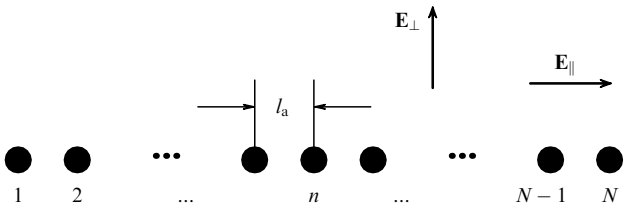

Figure 1. The geometry of the one-dimensional problem: the local field in an array of resonant atoms.The light wave propagates normally to the plane of the picture.

involving long-range dipole interactions, and hence that case falls outside the scope of our report.

We first consider a simpler problem of finding the local field in a one-dimensional array of atoms arranged along the z axis with equal interatomic distances l_a (Fig. 1). A laser beam, which is incident normally to the array, is polarized either along the array ($\mathbf{E}_{in} \parallel \hat{\mathbf{e}}_z$), thus inducing atomic dipole moments that are parallel to the array axis, or perpendicular to the array ($\mathbf{E}_{in} \perp \hat{\mathbf{e}}_z$), accordingly aligning the dipoles normally to the array and parallel to each other. In both cases, we have $\mathbf{E}_L \parallel \mathbf{E}_{in}$, and hence the equations for the field are reduced to scalar ones. Using the dimensionless variables $\mathcal{E}_n = [E_L(\mathbf{r}_n)/E_{in}]_{(p)}$, where $(p) = \parallel, \perp$ denotes the field polarization, we can write Eqn (1) for each polarization as

$$\mathcal{E}_n - \frac{\delta_R}{2(\delta + i)} \sum_{\text{chain}}^{j \neq n} \frac{\mathcal{E}_j/S}{|j-n|^3} = 1 , \tag{3}$$

where $1 \leqslant n, j \leqslant N$,

$$\delta_R = -4SF_{(p)} \frac{|d_a|^2 T}{\varepsilon \hbar l_a^3} , \tag{4}$$

and the summation in Eqn (3) is performed over all atoms in the one-dimensional array (chain), resulting in the appearance of the factor $S = \sum_{j=1}^{\infty} j^{-3} \approx 1.202$. The factor $F_{(p)}$ is defined by the field polarization, $F_\parallel = 1$ and $F_\perp = -1/2$. In the nearest-neighbor approximation, similarly to the Ising model for magnetic media, the summation over all atoms in Eqn (3) may be replaced with a simpler sum, $\mathcal{E}_{n-1} + \mathcal{E}_{n+1}$ (one can then set $S = 1$). In both cases [i.e., for the full summation in Eqn (3) and in the nearest-neighbor approximation], the results are qualitatively similar. In the case of a two-atom system, discussed below, the two approaches naturally merge.

As $N \to \infty$, a solution of Eqn (3) can be found as a sum of the uniform 'Lorentz' field

$$\bar{\mathcal{E}} = \frac{\delta + i}{\delta - \delta_R + i} \tag{5}$$

and wave contributions of the form $\Delta\mathcal{E} \propto \exp(\pm iqn)$. The wave number of each of these spatially oscillating solutions is $q = 2\pi l_a/\Lambda$, and the wavelength Λ, to be found later, is usually much shorter than the wavelength of the incident light. Here, we note an analogy to the phonon theory [4], except that our case involves not mechanical vibrations of atomic nuclei but excitations of bound electrons. The solution of Eqn (3) is very anisotropic, with a pronounced dependence on the polarization of the incident wave. The homogeneous 'Lorentz' component of the local field is significantly suppressed at the exact resonance, i.e., if the laser frequency is tuned to the frequency of the atomic transition, $\delta = 0$, and the dipole interaction between atoms is strong, $|\delta_R| \gg 1$:

$$|\bar{\mathcal{E}}_{res}|^2 = \frac{1}{1 + \delta_R^2} \ll 1 . \tag{6}$$

In this case, the field is essentially pushed out from the system. $|\bar{\mathcal{E}}|$ reaches its maximum at $\delta = \delta_R$,

$$|\bar{\mathcal{E}}_{peak}|^2 = 1 + \delta_R^2 \gg 1 . \tag{7}$$

The wave vectors q are found from the dispersion relation

$$\frac{1}{S} \sum_{n=1}^{\infty} \frac{\cos(nq)}{n^3} = \frac{\delta + i}{\delta_R} . \tag{8}$$

(In the nearest-neighbor approximation, the entire left-hand side of this equation may be replaced with $\cos q$.)

Within our present model, we showed that spatially oscillating solutions emerge if $|\delta_R| > 1$ in the range of frequency detunings $1 > \delta/\delta_R > -3/4$. (In the nearest-neighbor approximation, this range widens: $|\delta/\delta_R| < 1$.) The dipole strata are especially pronounced for $|\delta_R| \gg 1$. The strength of the dipole interaction between atoms may be gauged by the Rabi frequency $\Omega_R = \delta_R/T$, which essentially defines the position of the Lorentz resonance with respect to the atomic transition frequency. The Rabi frequency sets the width of the energy-spectrum band where locsitons can exist, such that for $|\delta_R| \gg 1$, this width is $\sim 2\hbar|\Omega_R| \gg \hbar\Gamma$. Here, we may draw some analogies with energy spectrum bands in solids [4] and in photonic crystals [12]. In the limit $1 - \delta/\delta_R \ll 1$ (i.e., on the band edge near the Lorentz resonance, where $\delta \approx \delta_R$), 'long-wave' locsitons emerge, with

$$q_{LW} \approx \sqrt{1 - \frac{\delta^2}{\delta_R^2}} , \tag{9a}$$

$$\Lambda_{LW} = \frac{2\pi l_a}{q_{LW}} . \tag{9b}$$

It is worth noting that their wavelength Λ_{LW} may be as large as $2\pi l_a \delta_R$, while remaining much shorter than the wavelength of the incident light wave. A typical example of such strata is presented in Fig. 2 (top curve). At the opposite edge of the locsiton frequency band (in the nearest-neighbor approximation, it corresponds to $1 + \delta/\delta_R \ll 1$), short-wave locsitons emerge with $q_{SW} \lesssim \pi$ and $\Lambda_{SW}/2 \gtrsim l_a$, which is close to the shortest spatial oscillation wavelength possible in a discrete system.

Because $\Lambda_{SW}/2$ is generally not a multiple of l_a, the distribution of dipole moments and the corresponding local fields in the discrete array of atoms may be spatially modulated with a longer wavelength, much like in the case of two waves with close wave vectors. Such modulation is clearly visible in the middle curve in Fig. 2, where $\Lambda_{SW}/2$ is quite close to l_a. The case of the exact resonance of the incident wave with the atomic transition, for which $\delta = 0$, may be used to divide the locsiton frequency band into the regions with short-wave and long-wave locsitons. The boundary case, with $\Lambda = 4l_a$, is represented by the lower curve in Fig. 2.

To draw an analogy with phonons, we note that long-wave locsitons are counterparts of acoustic phonons, and short-wave locsitons correspond to optical phonons. Another interesting analogy can be drawn with ferromagnetic or

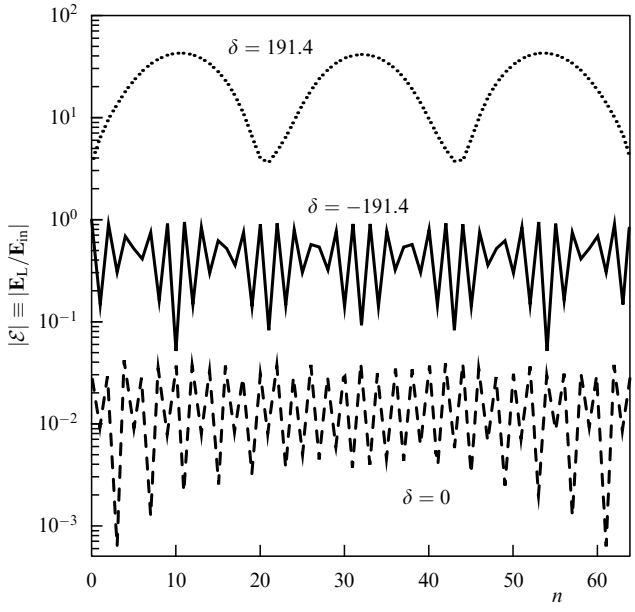

Figure 2. Dipole strata in an array of $N = 65$ atoms: the distribution of the absolute value of the local field at $\delta_R = 200$ at three different laser frequency detunings δ; n is a sequential number of an atom in the array.

ferroelectric materials, which feature strong interaction between static magnetic or electric dipoles. Within this analogy, the locsitons with the longest wavelengths resemble ferromagnets, while those with the shortest wavelengths resemble antiferromagnets. A similar analogy may also be noticed in the difference between bistability regimes in these two extreme cases, which we consider below for the simplest, two-atom, system.

We emphasize that this analogy between the locsitons and ferromagnets or ferroelectrics is inevitably very limited. For example, at $\delta = 0$, a hybrid configuration of a sort is formed by the induced atomic dipoles in the array, $\uparrow \circ \downarrow \circ \uparrow \cdots$, which corresponds to the lower curve in Fig. 2. Such hybrid configurations are only possible because of the dynamic nature of the atomic dipoles in our optical problem, and are unattainable with static dipoles. Thus, the dipole configuration in an array of atoms can be smoothly transformed from a 'ferromagnetic-like' to an 'antiferromagnetic-like' by tuning the laser frequency from one locsiton band edge to the other, while going through all the different hybrid configurations in the process.

We have shown that a finite array of atoms should exhibit size-related resonances, which are somewhat similar to resonances in thin semimetal films [13], long organic molecules [14], or a common violin string. The main difference is that in our case, the number of resonances is limited by the number of atoms N. The linear system of equations (3) may be solved, for example, by using numerical matrix solvers for $N \gg 1$, while for small N, the problem is amenable to analytic methods. Some results for the local field $\mathbf{E}_L$ obtained using numerical methods are shown in Figs 2 – 5.

We also used the following simple approximation to achieve a better qualitative understanding of the numerical results. The solution for an infinite array of atoms can be used to approximate the solution for a finite array of N atoms as a sum of the uniform 'Lorentz' solution $\bar{\mathcal{E}}$ at $N = \infty$ and spatially oscillating components $\Delta\mathcal{E} \propto \exp(\pm iqn)$, where the resonant locsiton wavenumber q and the resonant amplitude $\Delta\mathcal{E}$ are found from appropriate boundary conditions for the local field at the array ends. If the interaction between all atoms is taken into account, boundary conditions can only be approximated; however, we verified the precision of such an approximation for locsitons with sufficiently long wavelengths by many numerical simulations.

In the nearest-neighbor approximation, the method described above yields an exact solution of the problem. In this solution, the half-wavelength $\Lambda_1/2 = (N+1)\,l_a$ of the resonant locsiton with the longest wavelength is determined from the condition that the nodes of the local-field eigenmode lie beyond the end atoms of the array at the distances l_a, i.e., $\mathcal{E}_0 = \mathcal{E}_{N+1} = 0$. The frequency resonances for the locsitons are defined by the frequency detuning δ_k ($0 < k \leqslant N$):

$$\delta_k = \delta_R \cos q_k\,, \tag{10a}$$

where

$$q_k = \frac{\pi k}{N+1}\,. \tag{10b}$$

The corresponding locsiton wavelength is $\Lambda_k = \Lambda_1/k$. Due to symmetry considerations, only resonances with an odd k may be excited by an incident laser beam with a symmetric transverse field profile, while resonances with an even k may be excited by a beam with an antisymmetric profile. The solid curve in Fig. 3 depicts resonances of the maximum local field

$$\mathcal{E}_{max} \equiv \max_{0<n\leqslant N} |\mathcal{E}_n|$$

at the atoms in the array; the resonances are obtained in the nearest-neighbor approximation for a uniform distribution of the incident field along an array with $N = 13$ and $\delta_R = 200$. The lower envelope for this curve is $\mathcal{E}_{low}(\delta) \approx 2\bar{\mathcal{E}}$, while the

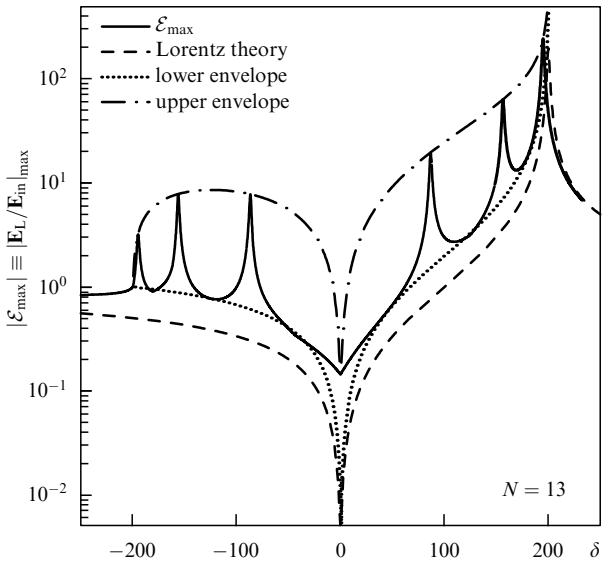

Figure 3. Locsiton resonances appearing in the dependence of the normalized maximum amplitude $\mathcal{E}_{max}$ of the local field on the laser frequency detuning δ in an array of $N = 13$ atoms with $\delta_R = 200$ (solid curve). For comparison, its upper and lower envelopes are shown, along with the corresponding dependence obtained using the classical Lorentz theory for unbounded media (the dashed curve).

upper envelope, obtained in the nearest-neighbor approximation, is given by

$$\mathcal{E}_{\rm up} \approx \begin{cases} \bar{\mathcal{E}}\left(n_\delta + \dfrac{1}{n_\delta}\right), & n_\delta \leqslant 1\,, \\ 2\bar{\mathcal{E}}, & n_\delta > 1\,, \end{cases} \tag{11a}$$

where

$$n_\delta = \frac{N+1}{2\sqrt{\delta_{\rm R}^2 - \delta^2}}\,. \tag{11b}$$

As N increases, the resonances start merging and become weaker as N approaches $\delta_{\rm R}$. However, even for large N, the lower envelope $\mathcal{E}_{\rm low}$ is still twice the local field $\bar{\mathcal{E}}$ predicted by the classical Lorentz theory [see Eqn (5)].

For $N = 3k - 1$, where k is a natural number, the local-field amplitude $\mathcal{E}_{\rm max}$, which is obtained in the nearest-neighbor approximation, goes below $\mathcal{E}_{\rm low}$ at $\delta = -\delta_{\rm R}/2$. For this frequency detuning δ, the absolute value of the locsiton wave number is $|q| \approx 2\pi/3$, and the spatial period of the locsiton is $\Lambda = 3l_{\rm a}$. The long-wavelength modulations of the spatial profiles of the dipole moments and the local field in the array disappear in this case because Λ becomes an integer multiple of $l_{\rm a}$. This results in an 'antiresonance' of a sort appearing in the dependence of the local field $\mathcal{E}_{\rm max}$ on δ; in other words, the locsiton in the array becomes suppressed.

Another important and unusual effect that we discovered is the cancelation of the resonant local-field suppression in an array consisting of a certain 'magic' number of atoms. At the exact resonance of laser radiation with the atomic transition (i.e., at $\delta = 0$) and for $|\delta_{\rm R}| \gg 1$, the local field obtained from the Lorentz theory is 'pushed out' of the system [see Eqn (6)]. We call this effect the resonant local-field suppression; it is also present in finite arrays of atoms for most N. We found, however, that at a certain magic number N, this resonant suppression vanishes, and the local field penetrates the system even at $\delta = 0$. In the nearest-neighbor approximation, the magic array sizes are $N = km_{\rm mag} + 1$, where k is a natural number and $m_{\rm mag} = 4$. The effect is most pronounced at $N = 5$, where the atomic dipoles arrange as $\uparrow \circ \downarrow \circ \uparrow$, with the amplitudes of the dipoles and the local field reaching their maxima ($\mathcal{E}_{\rm mag} \approx 1/3$) at odd-numbered atoms, while almost vanishing at even-numbered atoms. The 'magic enhancement' of the local field (compared to the uniform, Lorentz case) can be substantial: $|\mathcal{E}_{\rm mag}/\bar{\mathcal{E}}_{\rm res}| \approx \delta_{\rm R}/3$. In this effect, one of the resonant locsitons, whose frequency exactly matches that of the atomic transition, virtually compensates the resonant suppression of the local field in the system. The effect is also present if interactions between all atoms in the array are taken into account [see Eqn (3)], where $m_{\rm mag} = 13$. While an interference of an evil spirit cannot be excluded completely, we assume that the result stems from properties of the equation for the wave vector q of a locsiton in the array of atoms; this equation follows from Eqn (8) at $\delta = 0$:

$$\sum_{n=1}^{\infty} \frac{\cos(nq)}{n^3} = 0\,. \tag{12}$$

The smallest positive root q_1 of Eqn (12) is such that q_1/π is very close to a rational number, $(q_1/\pi)/(6/13) = 1.00026\ldots$, and hence the locsiton wavelength is $\Lambda = 2\pi/q_1 \approx (13/3)l_{\rm a}$, and a multiple of $\Lambda/2$ is therefore close to a multiple of $l_{\rm a}$. Therefore, the resonant local-field suppression is canceled at $N = 14$, with the relative amplitude of the field becoming substantial, $\mathcal{E}_{\rm mag} \approx 2/15$.

There is a semantic irony in that the local-field effects are actually due to nonlocal interactions between atoms. If the field of an incident wave is limited to a small spatial region, the local field can extend beyond this region; locsitons can propagate away from their origin. At the edges of the locsiton frequency band, i.e., at $|\delta_{\rm R}| > |\delta| \gg 1$, the group velocity of a locsiton $v_{\rm gr} \approx l_{\rm a}(\Omega_{\rm R}^2 - \Delta\omega^2)^{1/2}$ could be lower than the speed of sound in a solid. This effect can be useful, for instance, in designing nanometer-scale delay lines that could be used in molecular computers or integrated nanodevices for optical signal processing.

Aside from dipole strata, other even more interesting structures emerge in two-dimensional lattices of resonant atoms. For example, we consider a standing electromagnetic wave acting on an equilateral triangular lattice of atoms, the wave being polarized perpendicular to the lattice plane. The interatomic distances are very small, of the order of a few nanometers, and hence the external field can be regarded as uniform on a scale of several tens or even several hundred of atoms. We found that at certain conditions, concentric dipole strata (Fig. 4) can emerge around a circular hole made by removing several tens of atoms from the lattice; the amplitude of the strata decreases fast as the distance to the hole boundary increases. An even more interesting dipole configuration emerges if the laser radiation is incident normally to the lattice and polarized in the lattice plane. For better qualitative understanding of the local-field behavior in this case, we use the 'near-ring approximation,' which is a modification of the nearest-neighbor approximation: we consider interactions of each atom with its six immediate neighbors only, while assuming that the positions of the six atoms are evenly 'spread' over a circle with the diameter of one interatomic distance $l_{\rm a}$. As in the one-dimensional case, we introduce a polarization-independent dimensionless parameter $\tilde{\delta}_{\rm R}$, which differs from $\delta_{\rm R}$ defined by Eqn (4) in that we set $SF_{(p)} = -1$ here:

$$\tilde{\delta}_{\rm R} = \frac{|d_{\rm a}|^2 T}{\varepsilon\hbar l_{\rm a}^3}\,. \tag{13}$$

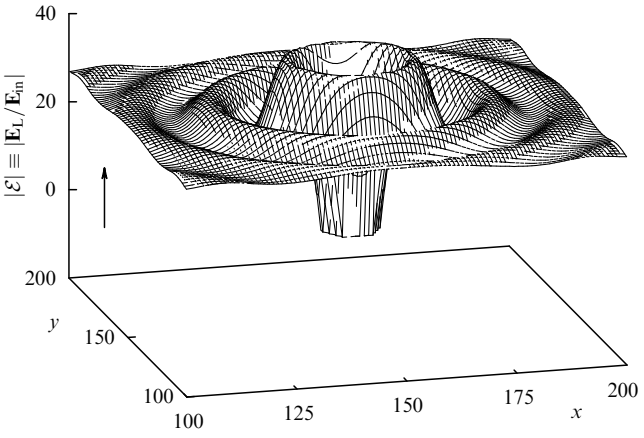

Figure 4. Localization of a locsiton in a two-dimensional triangular lattice of atoms around a hole with a diameter of 15 interatomic distances. The distribution of the local field $\mathcal{E}$ in the system is shown in the case where the external field of the light wave is normal to the lattice plane, $\delta = 100$, and $\tilde{\delta}_{\rm R} = 69$.

Comparing Eqns (2) and (4), we see that $Q = \tilde{\delta}_R/(\delta + i)$. After replacing the summation in Eqn (1) by an integration over the 'near ring' described above, we find a simple isotropic expression for the uniform Lorentz local field:

$$\bar{\mathbf{E}}_L = \frac{\mathbf{E}_{in}}{1 + (3/4)\,Q}\,. \tag{14}$$

It can be demonstrated that Eqn (14) remains valid not only in the near-ring approximation but also in the context of more precise calculations, which account for the structure of the two-dimensional lattice of atoms and for the dependence of the solution on the direction of the locsiton wave vector $\mathbf{q}$ within the first Brillouin zone. As in the one-dimensional case, we sought a solution of Eqn (1) as a superposition of the Lorentz field $\bar{\mathbf{E}}_L$ and plane-wave locsitons with the coordinate dependences $\exp(\pm i\mathbf{q}\mathbf{r}/l_a)$. Assuming that $\mathbf{q}$ makes an angle ψ with the polarization direction of the incident laser radiation, we arrive at the following dispersion relation for two-dimensional locsitons (which is a good approximation for relatively long-wavelength locsitons):

$$1 + \frac{3}{4}\,Q\left[J_0(q) - 3J_2(q)\cos(2\psi)\right] = 0\,, \tag{15}$$

where J_n is a Bessel function of the first kind.

The near-ring approximation becomes insufficient for short-wavelength locsitons; a more detailed study is required in this case, which takes account of the symmetry of the triangular lattice of atoms and the respective Brillouin zone structure. We have shown that the solution in this more general case depends on the orientation of the incident laser polarization with respect to the lattice. We let $\mathbf{u}_K$ denote the unit vector pointing from a given atom to one of its nearest neighbors (this corresponds to the ΓK direction in the first Brillouin zone). We consider four most interesting configurations defined by different polarizations and orientations of the locsiton wave vector:

a) $\mathbf{q} \perp \mathbf{E}_{in}$, $\mathbf{E}_{in} \parallel \mathbf{u}_K$,

b) $\mathbf{q} \perp \mathbf{E}_{in}$, $\mathbf{E}_{in} \perp \mathbf{u}_K$,

c) $\mathbf{q} \parallel \mathbf{E}_{in}$, $\mathbf{E}_{in} \parallel \mathbf{u}_K$,

d) $\mathbf{q} \parallel \mathbf{E}_{in}$, $\mathbf{E}_{in} \perp \mathbf{u}_K$.

The respective dispersion relations in these four cases are found by us to be

a) $\cos\dfrac{q\sqrt{3}}{2} = 4(1 + Q^{-1})$,

b) $\cos\dfrac{q}{2} = \dfrac{1}{8}\left[5 \pm \sqrt{57 + 64\,Q^{-1}}\right]$,

c) $\cos\dfrac{q}{2} = \dfrac{1}{16}\left[1 \pm \sqrt{1 + 128(1 - Q^{-1})}\right]$,

d) $\cos\dfrac{q\sqrt{3}}{2} = \dfrac{2}{5}(1 - 2Q^{-1})$.

The dipoles induced in a finite two-dimensional lattice form distinctive patterns if locsiton resonances emerge at the same Q in both dimensions. In the limit of long-wavelength locsitons ($q \ll 1$), the dispersion relations in cases (a) and (b) coincide with each other and with the result obtained in the near-ring approximation [see Eqn (15)]. In these two cases, $\psi = \pi/2$ and $Q \approx -4/3$, while

$$q_a^2 \approx q_b^2 \approx q_{ring}^2 \approx -\frac{32}{3}\left(\frac{3}{4} + \frac{1}{Q}\right). \tag{16}$$

In a similar manner, we obtain approximate solutions in cases (c) and (d), for which $\psi = 0$:

$$q_c^3 \approx q_d^2 \approx q_{ring}^2 \approx \frac{32}{15}\left(\frac{3}{4} + \frac{1}{Q}\right). \tag{17}$$

Combining cases (a) and (b) or cases (c) and (d), we can achieve simultaneous resonances in both directions in the lattice, if the lattice is approximately square in shape. Resonances of the same order are attained this way for locsitons with wave vectors pointing in two orthogonal directions; a sufficient 'squareness' of the two-dimensional triangular lattice can be achieved by choosing the lattice size (i.e., the numbers of atoms in the two directions). Locsitons with shorter wavelengths and wave vectors pointing in different directions are also present, but they do not significantly affect the emerging dipole pattern because of their nonresonant nature.

The interference of locsitons in a two-dimensional lattice of atoms can produce many different dipole excitation patterns and strata. Some of them are reminiscent of 'quantum carpets' [15]. Figure 5 depicts vector patterns that are formed by the atomic dipoles induced by the local field. The atoms are arranged in a 48×56 equilateral triangular lattice, which results in approximately equal sides of the lattice patch. The field of the incident electromagnetic wave is uniform and is polarized along the diagonal of the lattice patch. The incident wave frequency is chosen such that the third resonance (in the order of increasing wavenumbers, counting only the resonances allowed by the symmetry of the problem) is excited in each dimension; at least six distinct vortices of the local field are visible. Figure 5 shows the

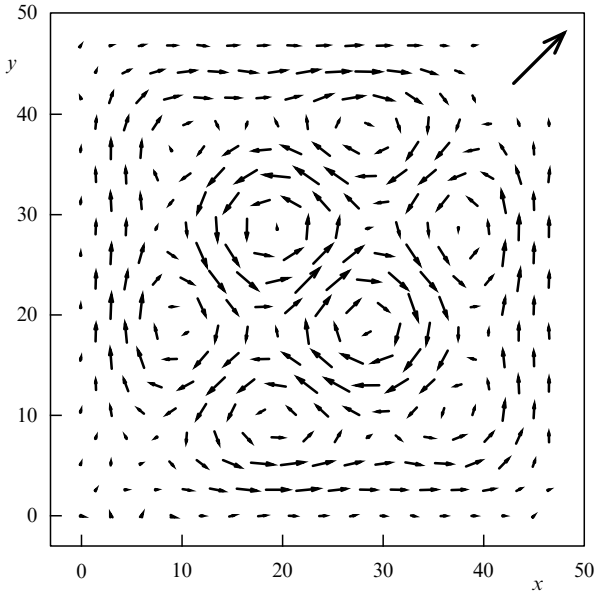

Figure 5. Vortices in the distribution of the local field $\mathcal{E}$ in a nearly square patch of a two-dimensional triangular lattice of atoms at $\delta = -1000$ and $\tilde{\delta}_R = 1316.5$. To avoid overcrowding of the plot, only one of each nine dipoles is shown. The incident light wave is polarized in the lattice plane along the diagonal of the lattice patch, its field shown by the large arrow.

imaginary parts of the complex field amplitudes, because they are dominant for each of the resonant locsitons.

Finite two-dimensional lattices and other similar systems of resonant atoms produce especially interesting examples of the cancelation of the resonant local-field suppression. Unlike in the one-dimensional arrays of atoms, the 'restoration' of the local field in such systems at $\delta = 0$, compared to that in the uniform, Lorentz case, can be more complete (up to 100%). The two-dimensional 'magic shapes' of atoms have the same 'cabbalistic' streak as in the one-dimensional case. For example, in the nearest-neighbor approximation, the effect is most pronounced only in the system of $N = 13$ atoms arranged as an equilateral six-point star with an atom at the center, for which the maximum restoration of the local field is reached, $\mathcal{E}_{\max} \approx 1.02$. The directions and relative amplitudes of the local field at the atoms in this system are shown in Fig. 6 for $\mathbf{E}_{\text{in}} \parallel \mathbf{u}_{\text{K}}$. It can be seen from the picture that the local field is concentrated on the outermost atoms and the one at the center, while the local field at the inner hexagon of atoms is almost completely suppressed. Any symmetry distortion in this system of strongly interacting atoms (e.g., by attaching a foreign atom or molecule to it) would break the balance of the local fields in the system and bring back the resonant suppression of the local field, which is canceled in the symmetric 'magic system.' This effect may be used, inter alia, in designing nanometer-scale sensors for detecting various biological molecules.

A sufficiently strong electromagnetic field applied to a system of strongly interacting atoms can bring about nonlinear local-field effects, e.g., solitons. A detailed consideration of many and varied interesting effects of this kind falls out of the scope of this report. It is worth noting, however, that some nonlinear effects, such as optical bistability and hysteresis, are possible even in the steady-state regime considered here, where the amplitude of the incident electromagnetic wave is constant. The optical bistability for the uniform, Lorentz local field in an unbounded medium was predicted in [16] and experimentally observed later in [17]. However, the possibility of bistability and multistability for short-wavelength locsitons, whose local field is highly nonuniform in space, has not been discussed in the literature. We found that this effect is possible even in the ultimately simple system of two two-level atoms with a saturation nonlinearity and a strong dipole interaction. This system also provides the most dramatic example of a self-induced local-field nonuniformity.

We describe the two-atom system using Eqns (3) and (4) with $S = 1$. Depending on the orientation of the local and external fields $\mathbf{E}_{\text{L}} \parallel \mathbf{E}_{\text{in}}$ either perpendicular or parallel to the line connecting the two atoms, Eqn (4) respectively includes either $F_{\perp}$ or $F_{\parallel}$. We introduce dimensionless amplitudes of the local field at each atom, $Y_j = E_j/E_{\text{sat}}$, where $j = 1, 2$, and the dimensionless field of the incident wave, $X = E_{\text{in}}/E_{\text{sat}}$, by normalizing the amplitudes of these fields to the saturation field E_{sat} of the two-level system. With this new notation, the system of equations for the local fields takes the form

$$Y_1 = X + \frac{\delta_{\text{R2}}(\delta - \text{i})\, Y_2}{1 + \delta^2 + |Y_2|^2}\,, \tag{18a}$$

$$Y_2 = X + \frac{\delta_{\text{R2}}(\delta - \text{i})\, Y_1}{1 + \delta^2 + |Y_1|^2}\,, \tag{18b}$$

where $\delta_{\text{R2}} \equiv \delta_{\text{R}}/2 > 0$. Equations (18) give rise to two types of solutions, or two different modes, for the local field in the system. A solution of the first type is similar to the uniform Lorentz solution for an infinite array of atoms, in which the local fields at the two atoms oscillate in phase. In this case, system of equations (18) leads to a cubic equation for $|\bar{Y}|^2$, which is readily solved or analyzed with the help of a plot, Fig. 7. For $|\delta_{\text{R2}}| \gg 1$, the onset of bistability and hysteresis for $\bar{Y}$ occurs at the detuning $\delta \approx \delta_{\text{R2}}$ of the laser frequency from the frequency of the two-level transition, with $\delta_{\text{R2}} - \delta > \sqrt{3}$. In this case, the threshold field of the incident wave $X_{\text{thr}} \approx [(2/\sqrt{3})^3/\delta_{\text{R2}}]^{1/2} \ll 1$, i.e., it may be significantly below the saturation field E_{sat} of the two-level system.

In the case of antiphase oscillations of local fields, a multistable solution of the second type is in fact the limit case of a short-wave locsiton that emerges at the opposite edge of the locsiton band at $\delta \approx -\delta_{\text{R2}}$. In the limit $|X| \ll \delta_{\text{R2}}$, in addition to the uniform, Lorentz local field $\bar{Y} \approx X/2$, we found a nonuniform solution

$$Y_{1,2} = \bar{Y} \pm s\,, \tag{19a}$$

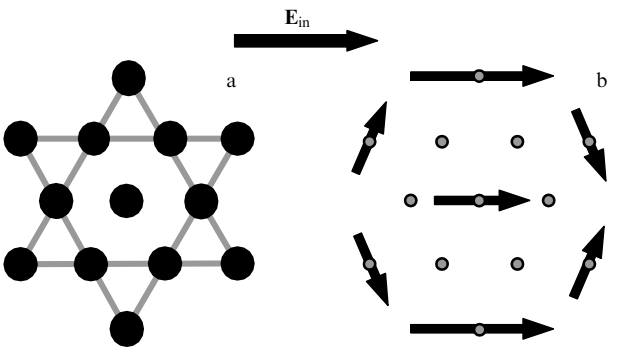

Figure 6. (a) The geometry of a 'magic system' of 13 resonant atoms; (b) the local field distribution in the system.

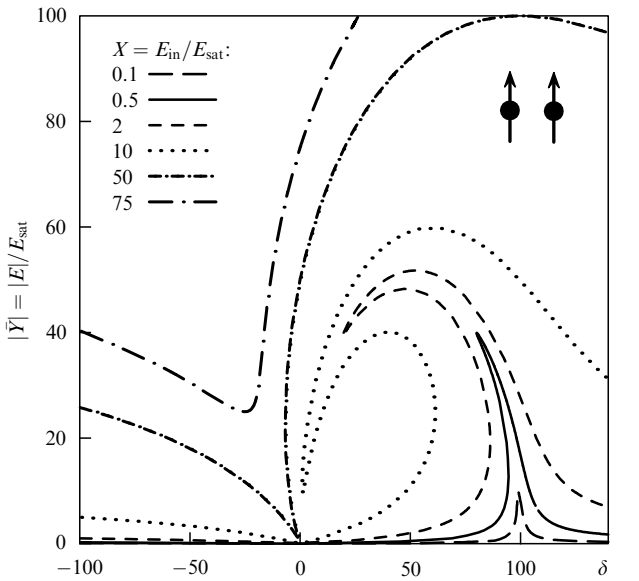

Figure 7. Optical bistability and hysteresis in a system of two resonant atoms with the saturation nonlinearity. The dependences of the normalized local-field amplitude $|\bar{Y}|$ on the frequency detuning δ are shown for $\delta_{\text{R2}} = 100$ and different normalized field amplitudes X of the incident wave.

where

$$s = \frac{\sigma}{\sqrt{2}} \left(\sqrt{1 \mp R} - \mathrm{i} \sqrt{1 \pm R} \right), \tag{19b}$$

$$\sigma = \sqrt{\delta_{\mathrm{R2}}(\delta_{\mathrm{R2}} + \delta) - 2\bar{Y}^2 \pm \bar{Y}^2 R}, \tag{19c}$$

$$R = \sqrt{1 - \frac{\delta_{\mathrm{R2}}^2}{\bar{Y}^4}}. \tag{19d}$$

The choice of the signs in Eqns (19b) and (19c) is independent of the choice of the sign in Eqn (19a). In Eqn (19a), one of the possible choices for the $\pm$ sign corresponds to Y_1 and the other corresponds to Y_2, which enables two different solutions, depending on the signs chosen. A similar property leads to the split-fork bistability for counterpropagating waves in a ring resonator [18]. The necessary conditions for the second-type multistable solution for the local field are $\delta_{\mathrm{R2}} + \delta > \sqrt{3}$ and $X^2 > 4\delta_{\mathrm{R2}}$. Three branches of the solution are seen in Fig. 8 near the bistability threshold: two stable branches given by Eqns (19) and one unstable 'Lorentz' solution $\bar{Y}$. For $\delta_{\mathrm{R2}} + \delta > 2$, there exist five different branches of the solution, but only two of them are stable. The antiphase oscillations of the dipole moments of the two atoms, which are represented by the term $\pm s$ in Eqn (19a), could be likened to a pair of spins one of which is aligned and the other counter-aligned with the applied magnetic field.

Returning to the above-mentioned similarities between the local-field behavior in a system of atoms and the behavior of spins in magnetic materials, we emphasize that our research is focused on the effects that are characteristic of fairly small systems of atoms, while studies of magnetic phenomena are typically aimed at finding averaged, 'thermodynamic' properties of sufficiently large systems. It is possible that our approach, which allowed us to predict giant resonances, magic numbers and shapes of atoms, etc., may allow exposing similar effects in nanometer-scale magnetic systems. The internal structure of locsitons and dipole strata emerges at the nanometer scale, with many interesting effects involving drastic changes of the local field even between neighboring atoms, i.e., at distances of the order of a few nanometers or less. Optical methods are ill-suited for resolving such small systems, and therefore the X-ray or electron-energy-loss spectroscopies, as well as an observation of the size-related optical resonances predicted by us, may become more promising methods for detecting locsitons experimentally.

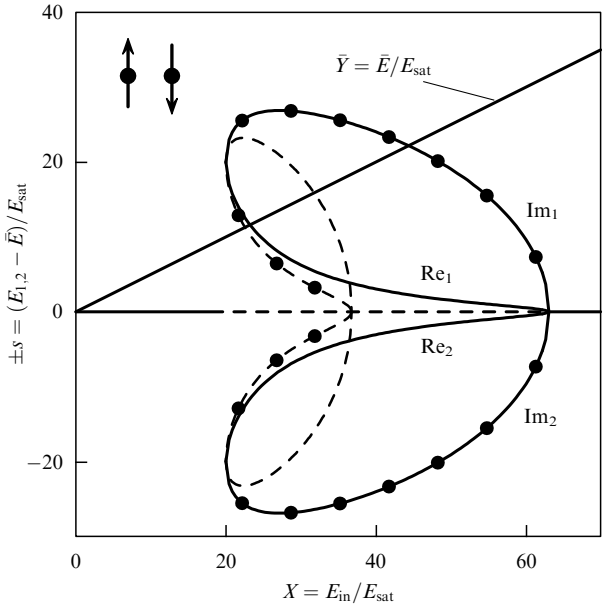

Figure 8. Optical bistability in the system of two resonant atoms with a saturation nonlinearity at $\delta_{\mathrm{R2}} = 100$ and $\delta_{\mathrm{R2}} + \delta = 10$. The thicker solid line represents the average uniform ('Lorentz') solution. The curves show the dependences of the 'nonuniform components' of our solution on the normalized field amplitude X of the incident wave. The solid and dashed curves respectively correspond to the stable and unstable regimes; the real parts of the solutions are shown with the curves marked with black dots, the imaginary parts are shown with the unmarked curves.

We note that locsitons and dipole nanostrata may open up fresh opportunities in designing elements for molecular computers and other nanodevices [19]. The significant advantage of locsitons over electrons in semiconductors and metals is that no electric current or charge transfer is required for locsitons to emerge. This advantage might aid in reducing the sizes of computer logic elements, since current semiconductor technology suffers from heat-related problems on a scale below 10 nm.

Locsitons might be put into service in both passive elements (e.g., for data transmission or in delay lines) and active elements (switches or logic elements). Locsiton-based nanodevices could thus supplement the list of alternative nanotechnologies, including plasmonics [20, 21], which is substantially based on surface plasmons [10, 11], and spintronics [22]. Another application of locsitons could be in nanosensors for biological molecules and other particles and impurities. Such a nanosensor may be built out of resonant receptor molecules, which can selectively bind target molecules or particles; otherwise, receptor molecules may be attached to particles with an optical resonance. By arranging the molecules in a magic shape, the nanosensor may be designed such that the locsiton in the system is not suppressed even at the exact resonance of the laser radiation with the constituent molecules; at the same time, the locsiton is to be suppressed whenever a target biological molecule attaches to the nanosensor.

Even more exciting opportunities open up in arrays and lattices of atoms with an inverse population of the resonant quantum transition; this inverse population may be created by an appropriate (e.g., optical) pumping. Such systems may open up the way to controlling locsitons, amplifying them, and even generating coherent locsitons with a 'locsiton laser' of a sort (a 'locster').

In conclusion, we demonstrated that dipole nanostrata and short-wave excitations of a local field (locsitons) can be brought about in arrays and lattices of strongly interacting atoms, including a two-atom system, by the action of laser radiation with a frequency close to that of the atomic resonance. Locsitonic effects include giant size-related resonances of the local field, the cancelation of the resonant local-field suppression in the system at certain magic shapes and numbers of atoms, and also optical bistability and hysteresis.

The authors are grateful to the US Air Force Office of Scientific Research (AFOSR) for funding this research.

References

1. Kaplan A E, Volkov S N *Phys. Rev. Lett.* **101** 133902 (2008)

2. Born M, Wolf E *Principles of Optics* 6th ed. (Oxford: Pergamon Press, 1980), (Chapter 2 and the references therein) [Translated into Russian: 2nd ed. (Moscow: Nauka, 1973)]
3. Aharoni A *Introduction to the Theory of Ferromagnetism* 2nd ed. (Oxford: Oxford Univ. Press, 2000)
4. Kittel Ch *Introduction to Solid State Physics* 7th ed. (New York: Wiley, 1996) [Translated into Russian (Moscow: Nauka, 1978)]
5. Bowden C M, Dowling J P *Phys. Rev. A* **47** 1247 (1993)
6. Maki J J et al. *Phys. Rev. Lett.* **67** 972 (1991)
7. Butylkin V S, Kaplan A E, Khronopulo Yu G *Zh. Eksp. Teor. Fiz.* **59** 921 (1970) [*Sov. Phys. JETP* **32** 501 (1971)]
8. Landau L D, Lifshitz E M *Teoriya Polya* (The Classical Theory of Fields) (Moscow: Nauka, 1988) [Translated into English (Oxford: Butterworth-Heinemann, 1980)]
9. Steel D G, Rand S C *Phys. Rev. Lett.* **55** 2285 (1985)
10. Shalaev V M et al. *Opt. Lett.* **30** 3356 (2005)
11. Markel V A, Sarychev A K *Phys. Rev. B* **75** 085426 (2007)
12. Yablonovitch E *Phys. Rev. Lett.* **58** 2059 (1987)
13. Sandomirskii V B *Zh. Eksp. Teor. Fiz.* **52** 158 (1967) [*Sov. Phys. JETP* **25** 101 (1967)]
14. Chernyak V, Volkov S N, Mukamel S *Phys. Rev. Lett.* **86** 995 (2001)
15. Kaplan A E et al. *Phys. Rev. A* **61** 032101 (2000)
16. Bowden C M, Sung C C *Phys. Rev. A* **19** 2392 (1979)
17. Hehlen M P et al. *Phys. Rev. Lett.* **73** 1103 (1994)
18. Kaplan A E, Meystre P *Opt. Commun.* **40** 229 (1982)
19. Heath J R, Ratner M A *Phys. Today* **56** (5) 43 (2003)
20. Murray W A, Barnes W L *Adv. Mater.* **19** 3771 (2007)
21. Fainman Y et al. *Opt. Photon. News* **17** (7) 24 (2006)
22. Žutić I, Fabian J, Das Sarma S *Rev. Mod. Phys.* **76** 323 (2004)

PACS numbers: **05.40. – a**, **05.45. – a**, 42.25.Dd, **46.65. + g**, 47.27.eb
DOI: 10.3367/UFNe.0179.200905j.0547

Modern methods for the statistical description of dynamical stochastic systems

V I Klyatskin

1. Introduction

S M Rytov gave much attention to the development of functional methods of stochastic system analysis at All-Moscow Radiophysics Seminars he led. He dubbed them *radiomathematics*. I participated in these seminars from the end of the 1960s. S M Rytov frequently asked, me in particular, a question: "What are you studying?" I traditionally answered that solutions of stochastic equations (ordinary and partial differential, or integral) are functionals from random coefficients of these equations and that I am studying the dependence of the statistical characteristics of these solutions on various models and the statistical parameters of these coefficients. For about 30 years I considered this answer to be exhaustive, and only during the last 10 – 15 year did I realize all the topicality of the question "What are you studying?" and the total inadequacy of my usual answer. This is related to the fact that in recent years the attention of both theorists and experimenters has focused on the question of the links of dynamics pertaining to averaged characteristics of problem solution to the solution behavior in specific realizations. This is especially relevant to geophysical problems related to the atmosphere and ocean in which, by and large, the respective averaging ensemble is absent and experimenters as a rule deal with individual realizations. In this case, the results of statistical analysis frequently not only have nothing in common with the behavior of solutions in specific realizations but often simply contradict them. It is namely this that I would like to demonstrate in this report.

Three approaches are currently utilized in the analysis of a stochastic dynamical system.

The first approach is based on analyzing the Lyapunov stability of solutions to deterministic linear ordinary differential equations

$$\frac{\mathrm{d}}{\mathrm{d}t}\,\mathbf{x}(t) = A(t)\;\mathbf{x}(t)$$

and traditionally attracts the attention of many researchers. One analyzes here the upper bound of the problem solution

$$\lambda_{\mathbf{x}(t)} = \overline{\lim_{t\to+\infty}}\;\frac{1}{t}\ln\left|\mathbf{x}(t)\right|,$$

which is termed its characteristic exponent. When this approach is applied to stochastic dynamical systems, it is common that, to interpret and simplify the obtained results at the final stage, statistical analysis is invoked and statistical averages such, for example, as

$$\left\langle\lambda_{\mathbf{x}(t)}\right\rangle = \overline{\lim_{t\to+\infty}}\;\frac{1}{t}\left\langle\ln\left|\mathbf{x}(t)\right|\right\rangle,$$

are computed.

The drawbacks of this approach to stochastic dynamical systems are as follows:

(1) Such simplifying features of random parameters as stationarity in time, homogeneity, and isotropy in space are exploited only at the stage of final analysis.

(2) When passing to continual generalizations of ordinary differential equations (for example, in mechanics or the electrodynamics of continuous media), i.e., to partial differential equations (to fields), the analysis of Lyapunov stability is only possible through the series expansions of solutions in complete sets of orthogonal functions. If such a technique is applied to stochastic problems, a question emerges as to whether the operations of series expansion and statistical averaging are permutable. In particular, when statistical characteristics of random processes and fields are approximated by singular (generalized) functions (as, for example, in the approximation that fluctuations of system parameters are delta-correlated), these operations are not, as a rule, permutable.

The second approach is also traditional and relies on the analysis of moment and correlation functions of solutions to stochastic problems.

The drawback of this second approach is that commonly used methods of statistical averaging smooth the qualitative features of separate realizations and it is not uncommon for the obtained statistical characteristics to have nothing in common with the behavior of separate realizations.

In certain circumstances there exist, however, physical processes and phenomena occurring with the probability of one (i.e., happening in almost all realizations). They are called *coherent* (see monographs [1 – 4] and work [5] where this question is thoroughly discussed). To describe such phenomena, the third approach is applied. It is rooted in *the method of statistical topography* which studies, instead of moment functions, the statistical characteristics of some functionals describing precisely these coherent phenomena.

Below, we will illustrate these approaches as applied to simple physical problems.